AGU PUBLICATIONS

JGR

Journal of Geophysical Research: Biogeosciences

RESEARCH ARTICLE
10.1002/2013JG002358

Key Points:
- Strong seasonality in TSM and POC fluxes
- Significant downstream changes in sediment and OC fluxes
- Floodplains are a likely candidate in regulating transport

Supporting Information:
- Readme
- Table S1

Correspondence to:
F. Tamooh,
fltamooh@yahoo.com

Citation:
Tamooh, F., F. J. R. Meysman, A. V. Borges, T. R. Marwick, K. Van Den Meersche, F. Dehairs, R. Merckx, and S. Bouillon (2014), Sediment and carbon fluxes along a longitudinal gradient in the lower Tana River (Kenya), *J. Geophys. Res. Biogeosci.*, *119*, 1340–1353, doi:10.1002/2013JG002358.

Received 6 APR 2013
Accepted 15 JUN 2014
Accepted article online 18 JUN 2014
Published online 18 JUL 2014

Sediment and carbon fluxes along a longitudinal gradient in the lower Tana River (Kenya)

Fredrick Tamooh[1,2], Filip J. R. Meysman[3,4], Alberto V. Borges[5], Trent R. Marwick[1], Karel Van Den Meersche[3,4], Frank Dehairs[3], Roel Merckx[1], and Steven Bouillon[1]

[1]Department of Earth and Environmental Sciences, Katholieke Universiteit Leuven, Leuven, Belgium, [2]Kenya Wildlife Service, Mombasa, Kenya, [3]Department of Analytical, Environmental, and Geo-Chemistry, Vrije Universiteit Brussel, Brussel, Belgium, [4]Royal Netherlands Institute of Sea Research, Yerseke, Netherlands, [5]Unité d'Océanographie Chimique, Université de Liège, Liège, Belgium

Abstract We estimated annual fluxes of suspended matter and different carbon (C) pools at three sites along the lower Tana River (Kenya), based on monthly sampling between January 2009 and December 2011. Concentrations of total suspended matter (TSM), particulate organic carbon (POC), dissolved organic carbon (DOC), and dissolved inorganic carbon (DIC) were monitored, as was the stable isotope composition of the carbon pools. Both TSM and POC concentrations showed strong seasonality, varying over several orders of magnitude, while DOC and DIC concentrations showed no seasonal variations. A strong shift in the origin of POC was observed, which was dominated by C3-derived C during dry conditions (low $\delta^{13}C_{POC}$ between −28‰ and −25‰), but had significant C4 contributions during high-flow events ($\delta^{13}C_{POC}$ up to −19.5‰). Between Garissa and the most downstream sampling point, a clear decrease in suspended matter and organic C fluxes was observed, being most pronounced during high-discharge conditions: on an annual basis, fluxes of TSM, POC, and DIC decreased by 34% to 65% for the 3 year study period. Our results suggest that floodplains along the lower Tana River could play an important role in regulating the transport of suspended matter and organic C. A comparison of current flux estimates with data collected prior to the construction of several hydropower dams reveals that the sediment loading is reduced during low discharge conditions.

1. Introduction

Fluvial systems are a key link between the terrestrial biosphere and the ocean, discharging ~36,000 $km^3\ yr^{-1}$ of water and ~20×10^9 $t\ yr^{-1}$ of sediment to the world coastal oceans [*Milliman*, 2001; *Milliman and Farnsworth*, 2011]. Rivers also transport about 0.9 Pg C yr^{-1} into the coastal ocean, of which ~56% is dissolved inorganic carbon (DIC) and the remainder consists of approximately equal contributions of particulate organic carbon (POC) and dissolved organic carbon (DOC) [*Ludwig et al*., 1996; *Schlünz and Schneider*, 2000]. The accurate quantification of global riverine C fluxes remains a challenge due to a lack of comprehensive data sets [*Richey*, 2004]. To better constrain C export to the coastal ocean, reliable information on spatial and temporal variations in C loadings for river basins in a representative range of climate and geographical settings are critical [*Schlünz and Schneider*, 2000; *Richey*, 2004].

On a global scale, and comparing different systems, the riverine fluxes of different compounds are controlled by different sets of environmental factors. The total suspended matter (TSM) flux to the coastal zone is best predicted by the basin area, slope, temperature, runoff, lithology, and human activities [*Ludwig et al*., 1996; *Syvitski and Milliman*, 2007]. POC fluxes are generally considered to be tightly correlated to TSM fluxes, based on the observation that the relative contribution of POC to the total particulate matter pool (%POC decreases with increasing TSM concentrations due to dilution of POC with mineral matter [*Ludwig et al*., 1996]. The riverine DOC flux is largely controlled by discharge, basin slope, soil C content as well as basin vegetation cover [*Ludwig et al*., 1996], whereas DIC fluxes are primarily a function of basin lithology, with carbonate mineral-rich basins generating high alkalinity and DIC export [*Cai et al*., 2008].

The transport of C in fluvial systems is not passive, as significant transformations can occur on the way to the ocean, with reservoirs and floodplains acting as hot spots for regulating riverine C dynamics [*Cole et al*., 2007]. For example, the transport and fate of POC is tightly linked to the movement of sediments, which can be deposited and remobilized several times in floodplains over varying time scales [*Richey*, 2006]. In this

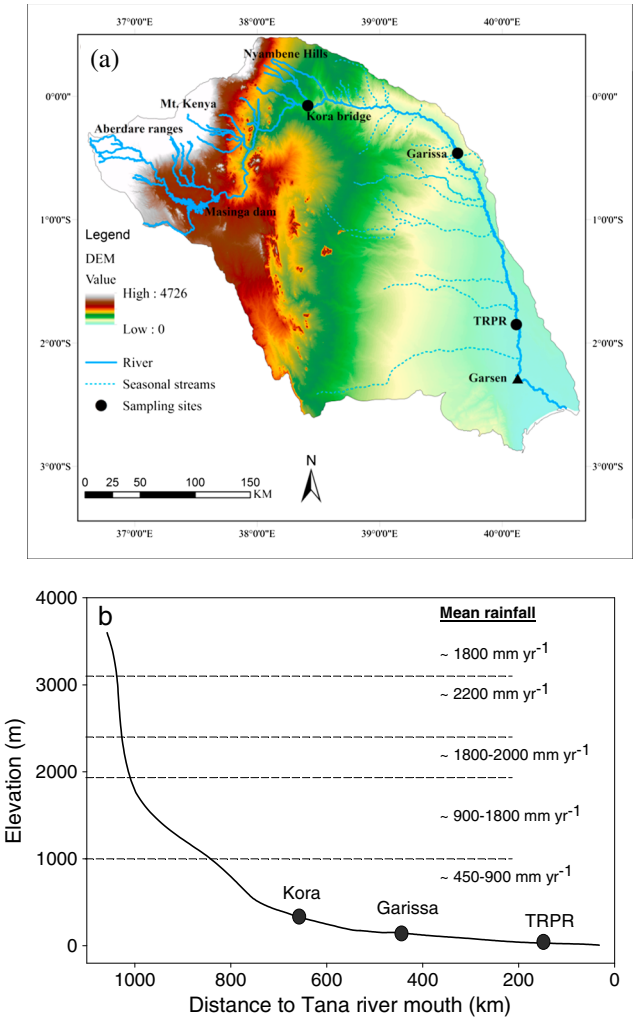

Figure 1. (a) Digital elevation model of the Tana River basin showing the three sampling sites. (b) Elevation profile showing sampling sites and mean annual rainfall range.

dynamic process, floodplains play a critical role for POC storage and processing. However, there are only a few studies quantifying the exchange of riverine sediments and C in large floodplains, despite the important role these ecosystems play in regulating the downstream transport [*Noe and Hupp*, 2009; *Zurbrügg et al*., 2013]. In turn, the transport of sediments and associated nutrients is considered to be vital for floodplain ecosystem functioning, with significant adverse effects imposed by hydropower dam construction and flood control management [*Maingi and Marsh*, 2002]. Within the flood pulse concept of *Junk et al*. [1989], floodplains have a strong influence on the riverine C dynamics via lateral linkages. Floodplains may act as either a sink or source of C to the riverine network depending on the balance between the longitudinal transport of C from the catchment and the lateral exchange of C between floodplains and river channels [*Alin et al*., 2008; *Hoffmann et al*., 2009; *Zurbrügg et al*., 2013].

The goal of the present study is an improved quantification of riverine fluxes of suspended sediments and C pools (POC, DOC, and DIC) in the Tana River basin. The Tana is the longest river in Kenya (~1100 km), with a total catchment area of ~96,000 km^2 (Figure 1a). In recent decades, a series of hydroelectric dams have been installed in the upstream reaches, which are thought to retain a substantial fraction of the sediment input from the upper catchment. This anthropogenic impact on the sediment dynamics is expected to further increase by newly planned irrigation and damming schemes. While earlier studies have explored the distribution and origin of sediments and C pools throughout the Tana Basin [*Bouillon et al*., 2009; *Tamooh et al*., 2012], annual sediment and C fluxes remain poorly constrained. Historical data on sediment loads are available for the city of Garissa [*Dunne*, 1988] and are representative of conditions prior to the construction of several reservoirs upstream of the Tana River. These reservoirs have acted as a significant sediment trap [*Dunne and Ongweny*, 1976; *Brown and Schneider*, 1998] and have been shown to affect the downstream riverine and floodplain ecosystems [*Maingi and Marsh*, 2002]. *Kitheka et al*. [2005] estimated TSM and POC transport at Garsen (Figure 1a), but this study was based on a limited data set and monthly averaged discharge data.

Here we present results from a 3 year study (January 2009 to December 2011) collecting monthly samples at three sites along the lower Tana River (Kora Bridge, Garissa, and Tana River Primate Reserve (TRPR), which are located ~655 km, ~455 km, and ~152 km from the Tana River mouth, respectively; Figure 1b). The lower Tana River has extensive floodplains but no perennial tributaries, allowing us to evaluate the possible role of floodplains as sources or sinks of suspended sediments and organic C. Besides the measurements of TSM concentrations and different C pools, we determined stable C isotope ratios ($\delta^{13}C$) to determine the origin of

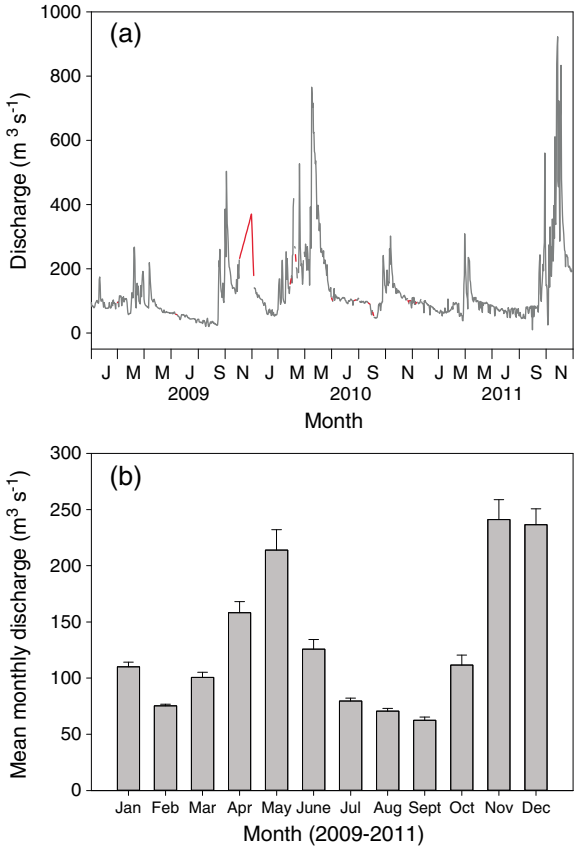

Figure 2. (a) Daily discharge (red sections highlight missing data gaps corrected by interpolation) and (b) mean monthly discharge data for Garissa during the three sampling years 2009–2011. The error bars in Figure 2b represent the standard deviation of the monthly discharge over the study period.

C and its seasonality. The lower catchment is typically characterized by riparian vegetation consisting of C3 plants, while beyond the riparian zone, the vegetation has strong contributions of C4 plants. Hence, variations in stable isotope signatures could provide information on the relative contributions of different parts of the catchment to the total C export.

2. Materials and Methods

2.1. Study Area

The Tana river system can be separated into two main parts, here referred to as "Tana headwaters" and "lower main Tana." The Tana headwaters consist of small mountainous streams emanating from the Aberdare Ranges in the central highlands of Kenya, the highlands around Mount Kenya, and the Nyambene Hills in eastern Kenya (Figure 1a). The lower main Tana encompasses the section downstream of the Nyambene Hills, where the river flows southeast for about 700 km through semiarid plains. Along this stretch, tributaries only discharge in short pulses during the wet season. As a result, the lower main Tana forms a single channel during the dry season, transporting material to the Indian Ocean [*Maingi and Marsh*, 2002]. The lower main Tana dissects extensive floodplains between the towns of Garissa and Garsen, but floodplain inundation has become more irregular in recent decades due to up streamflow regulation by five hydroelectric dams [*Maingi and Marsh*, 2002]. The reservoirs in the upper Tana have a combined surface area of 150 km^2, with a significant quantity of sediment reported to be trapped within these dams [*Dunne and Ongweny*, 1976; *Brown and Schneider*, 1998]. The Tana River basin includes various ecological zones experiencing different rainfall patterns, with annual precipitation strongly decreasing from the high-altitude forests to the semiarid catchment of the lower main Tana to the lower semiarid Tana catchment [*Brown and Schneider*, 1998] (Figure 1b). The basin experiences a bimodal hydrological cycle, with long rains between March and May, and short rains between October and December, which also leads to a clear bimodal pattern in the river discharge (Figures 2a and 2b). The mean annual river discharge at the Garissa gauging station is 156 $m^3 s^{-1}$ over the period 1934 to 1975 (daily data from the Global River Discharge Database, available at http://daac.ornl.gov/RIVDIS/rivdis.shtml). The high-altitude headwaters (Aberdare Ranges and Mount Kenya) are characterized by mountainous forest vegetation and moorlands at the highest elevations, which give way to more intense agricultural activities in midaltitude regions. The semi-arid lower Tana is dominated by open to wooded savannah grassland, with riverine gallery forests along the river. The drainage area upstream of Kora Bridge, Garissa, and TRPR is approximately 23%, 36%, and 69% of the total Tana River basin, respectively.

2.2. Sampling and Analytical Techniques

Water samples were taken from midstream using a bucket from bridges (Kora Bridge and Garissa Bridge) or from a boat (TRPR). Samples for TSM were obtained by filtering a known volume of water on preweighed 47 mm GF/F filters (0.7 μm; precombusted overnight at 450°C), which were subsequently dried and reweighed. After determining TSM, the same filters were used for further analysis of POC, particulate

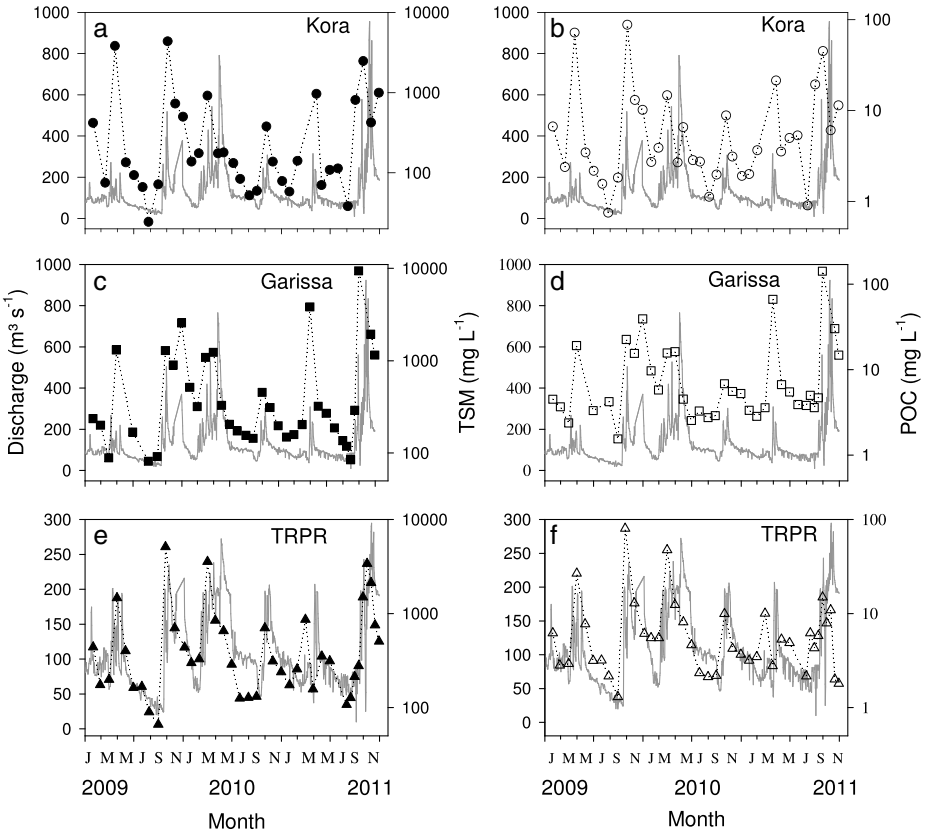

Figure 3. Seasonal variation of daily discharge (full lines) and TSM and POC (individual symbols and dotted lines) at the three sampling sites ((a and b) Kora, (c and d) Garissa, and (e and f) TRPR = Tana River Primate Reserve).

nitrogen (PN), and $\delta^{13}C_{POC}$. Filters were decarbonated with HCl fumes for 4 h, redried, and packed into Ag cups. POC, PN, and $\delta^{13}C_{POC}$ were determined on a Thermo elemental analyzer–isotope ratio mass spectrometer (EA-IRMS: FlashHT with DeltaV Advantage), using the TCD signal of the EA to quantify PN, and by monitoring *m/z* 44, 45, and 46 on the IRMS. Quantification and calibration of $\delta^{13}C$ data were performed with International Atomic Energy Agency (IAEA)-C6 and acetanilide that was calibrated against international standards. Reproducibility of $\delta^{13}C_{POC}$ measurements was typically better than 0.2‰.

Samples for DOC and $\delta^{13}C_{DOC}$ were obtained by prefiltering surface water through precombusted GF/F filters (0.7 μm), with further filtration through 0.2 μm syringe filters and preservation with H_3PO_4 in glass vials with Teflon-coated screw caps. DOC and $\delta^{13}C_{DOC}$ were measured with a customized Thermo HiperTOC coupled to a Delta + XL IRMS. A number of samples for DOC and $\delta^{13}C_{DOC}$ were lost or contaminated, resulting in a reduced data set for these parameters.

Water samples for total alkalinity (TA) analysis were obtained the same way as DOC samples, but no preservative was added. TA was analyzed by automated electrotitration on 50 mL samples with 0.1 mol L^{-1} HCl as titrant (reproducibility estimated as typically better than ±3 μmol kg^{-1} based on replicate analyses). DIC concentrations (mmol L^{-1}) were not determined analytically but estimated from an empirical relationship with alkalinity (mmol L^{-1}):

$$DIC = 1.0256 \times TA \quad (1)$$

This relationship was based on an independent TA and DIC data set from the lower main Tana obtained in three field campaigns encompassing different seasons [*Bouillon et al.*, 2009; *Tamooh et al.*, 2013]. In general, DIC showed a strong linear dependence on alkalinity ($r^2 = 0.997$; $n = 146$), indicating that TA can be used as a reliable predictor of DIC. For the analysis of $\delta^{13}C_{DIC}$, a 2 mL helium (He) headspace was created, and H_3PO_4

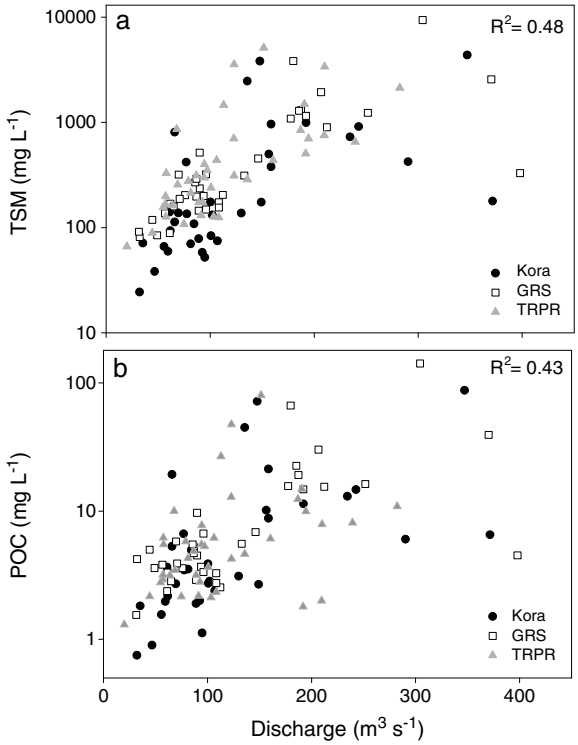

Figure 4. Relationship between (a) TSM concentrations and discharge and (b) POC concentrations and discharge at the three sampling sites (Kora = Kora Bridge, GRS = Garissa, and TRPR = Tana River Primate Reserve).

was added to convert all the DIC species to CO_2. After overnight equilibration, part of the headspace was injected in the carrier gas stream of an EA-IRMS (ThermoFinnigan Flash HT and ThermoFinnigan DeltaV Advantage) for $\delta^{13}C$ measurements. The resulting $\delta^{13}C$ data were corrected for the isotopic equilibration between gaseous and dissolved CO_2 as described by *Gillikin and Bouillon* [2007]. Measurements were calibrated with certified reference materials LSVEC and either NBS-19 or IAEA-CO-1.

The discharge between January 2009 and December 2011 at the Garissa station (Figure 2a) was based on daily measurements by the Water Resources Management Authority Kenya (WRMA). These daily discharge records showed a number of gaps (60 days over the 3 year sampling period, 2009–2011); these missing data were estimated by linear interpolation. For the Kora Bridge and TRPR sites, no discharge data were available, although such data are critical to estimate TSM and C fluxes. Discharge rates at these two sites were estimated from the Garissa data using an empirical flood propagation model, calibrated for the Tana Basin [*DHV*, 1986].

$$Q(t) = \min[Q_G(\text{t-tau}), 0.5\times(Q_G(\text{t-tau}) - Q_L)\times \tanh((y - y_1)/y_2) + 0.5\times(Q_G(\text{t-tau}) + Q_L)] \quad (2)$$

In this, $Q_G(t)$ represents the flow rate at Garissa at time t, Q_L is a reference discharge (190 m^3 s^{-1}), and τ is the estimated time lag between the site and Garissa (−2.5 days for Kora Bridge and 5 days for TRPR), while y_1 (200 km) and y_2 (130 km) are the distance parameters, and y is the distance from the river mouth (Kora: 600 km and TRPR: 80 km as determined in ArcGIS). This empirical flood flow attenuation model was calibrated using the daily flow data between 1941 and 1986 from Garissa and Garsen stations [*DHV*, 1986]. Recent measurements with an acoustic Doppler current profiler (River Ray) suggest that this historical rating curve is still sufficiently accurate for the purpose of this study (N. Geeraert, unpublished data).

The annual mean fluxes of TSM, POC, DOC, and DIC were estimated and compared using both GUMLEAF v1.0 (available at http://www.environmetrics.net.au/index.php?p=2_2) and LOADEST (available at http://water.usgs.gov/software/loadest/) software packages. GUMLEAF uses 22 different algorithms to calculate annual mean fluxes and their uncertainty from time series of constituent concentration and discharge data [*Tan et al.*, 2005]. The different GUMLEAF algorithms result in similar estimates (coefficients of variation were between 3 and 12% for dissolved fluxes (DIC and DOC) and between 10 and 36% for particulate fluxes (TSM, POC, and PN)). The flux calculations here are based on GUMLEAF algorithm 5 (annual flow-weighted mean concentration) and 19 (flow regime-stratified, flow-weighted mean concentration), because they generated low uncertainty estimates for our data set and because the mean values produced by these two methods were highly comparable (within 5% standard error). LOADEST is a FORTRAN program that uses the time series of discharge data and load concentrations to generate a regression model that predicts annual fluxes as a function of explanatory variable (discharge data). The LOADEST calibration and estimation procedures are based on three different statistical procedures: adjusted maximum likelihood estimation, maximum likelihood estimation, and least absolute deviation [*Runkel et al.*, 2004]. The first two methods are appropriate when the model errors are normally distributed. We used the first two methods since the data were normally distributed, and the flux estimates for the two methods were highly comparable (<4% standard error).

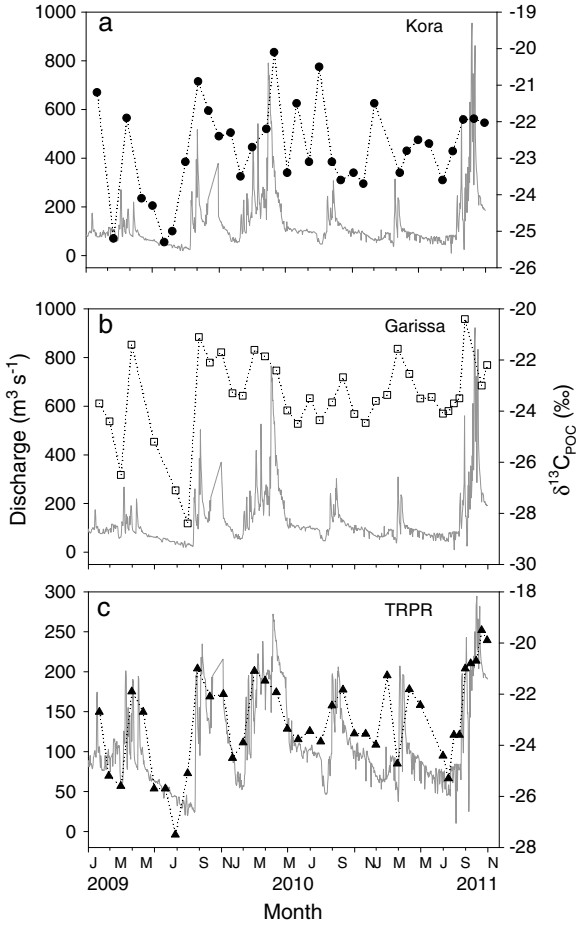

Figure 5. Seasonal variation of the daily discharge against $\delta^{13}C_{POC}$ values at the three sampling sites ((a) Kora = Kora Bridge, (b) GRS = Garissa, and (c) TRPR = Tana River Primate Reserve).

The true uncertainty of our fluxes is difficult to constrain; hence, we focus our analysis and interpretation on relative difference between fluxes rather than absolute flux values. Improved flux estimates for systems with an irregular hydrology such as the Tana will likely require data acquisition at higher temporal resolution than the monthly frequency employed here (i.e., ideally, the time interval between chemistry sampling points should be lower than the ~7 day residence time of the lower main Tana system).

3. Results

3.1. Discharge

Daily discharge at the Garissa gauging station ranged from 10 to 922 $m^3 s^{-1}$ over the 3 years of our study (Figure 2a and Table S1 in the supporting information) with a 3 year mean of 132 $m^3 s^{-1}$. The mean annual flow rate varied significantly ($p < 0.01$), with 2010 recording the highest value (158 $m^3 s^{-1}$), 2011 was an intermediate year (130 $m^3 s^{-1}$), and 2009 recorded the lowest value (110 $m^3 s^{-1}$). The monthly discharge data averaged over the three sampling years show a clear bimodal pattern, reflecting the long rainny season from March to June and the short rains in November–December (Figure 2b). High-flow regimes ($Q > 250\ m^3 s^{-1}$) only occurred infrequently during short pulses; 91% of our sample collection took place during low-flow regime ($Q \leq 250\ m^3 s^{-1}$). The discharge values at Kora, as calculated by the flood propagation model, were almost identical to those of Garissa, whereas the estimated flow values at the TRPR station were lower and particularly dampened during peak flows. The ratios between highest and lowest flow rates were high at Kora Bridge (93.8) and Garissa (90.6) compared to TRPR (21.8). The attenuation of peak flows between Garissa and TRPR (as predicted by the flood propagation model) is consistent with the modulation of river flows by the extensive floodplains along this river stretch.

3.2. Seasonal and Longitudinal Variations in Different C Pools

The monthly variations of both TSM and POC are presented in Figure 3. Overall, TSM ranged from 24 to 9386 mg L^{-1} across the three stations, while POC concentrations ranged from 0.8 to 141.9 mg C L^{-1} (Table S1 in the supporting information). The highest TSM concentration (9386 mg L^{-1}) was recorded at Garissa during a peak flooding event in October 2011. Both TSM and POC showed a consistent variation with discharge (Figure 3): TSM and POC concentrations showed a positive correlation with flow (Pearson's correlation, $p < 0.01$; $r^2 = 0.48$ and 0.43, respectively; Figure 4), but maximum concentrations clearly preceded peak discharge at all sites.

The DOC concentrations ranged from 0.8 to 5.2 mg C L^{-1} with an overall mean of 2.2 mg C L^{-1} across the three sites (Table S1 in the supporting information). At the three stations, DOC concentrations did not show a clear correlation with discharge, even though high values were typically recorded during high-flow periods. However, DOC concentrations at TRPR showed a positive correlation with TSM concentration (Pearson's correlation, $p < 0.05$; $r^2 = 0.51$). Overall, DOC concentrations decreased downstream, with a mean annual value of 2.9 ± 1.1 mg C L^{-1} at Kora Bridge, 2.1 ± 0.7 mg C L^{-1} at Garissa, and 1.7 ± 0.3 mg C L^{-1} (analysis of

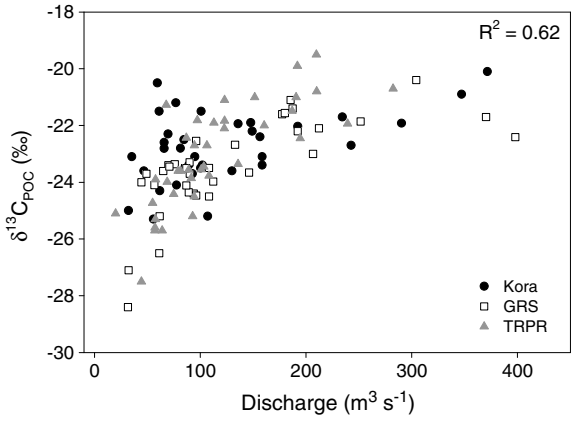

Figure 6. Relationship between $\delta^{13}C_{POC}$ signatures against discharge at the three sampling sites (Kora, Garissa, and TRPR = Tana River Primate Reserve).

variance (ANOVA), $p < 0.01$) at TRPR (all errors are reported as standard deviations unless specified otherwise). The reduction in DOC concentrations downstream was more pronounced during the wet season (~60% decrease) than during the dry season (~40% reduction).

The DIC concentrations ranged from 7.1 to 23.5 mg C L^{-1} and showed no clear variation with discharge (Figure 7 and Table S1 in the supporting information). However, the values increased consistently downstream (ANOVA, $p < 0.01$) with Kora Bridge recording an annual mean of 12.2 ± 2.9 mg C L^{-1}, Garissa 14.0 ± 3.3 mg C L^{-1}, and TRPR 16.1 ± 2.2 mg C L^{-1}.

The percentage of POC in the TSM (%POC) ranged from 0.2% to 5.2%, with higher values occurring during low-flow periods (ANOVA, $p < 0.01$; Table S1 in the supporting information). The %POC decreased downstream with mean values at Kora Bridge 2.5 ± 0.9%, Garissa 2.0 ± 0.8%, and TRPR 1.6 ± 0.7% (ANOVA, $p < 0.01$). Molar C:N ratios of organic matter ranged from 5.2 to 12.4 and were low during low-flow conditions and vice versa. The average C:N ratio at the three sites differed significantly (ANOVA, $p < 0.01$) with Kora

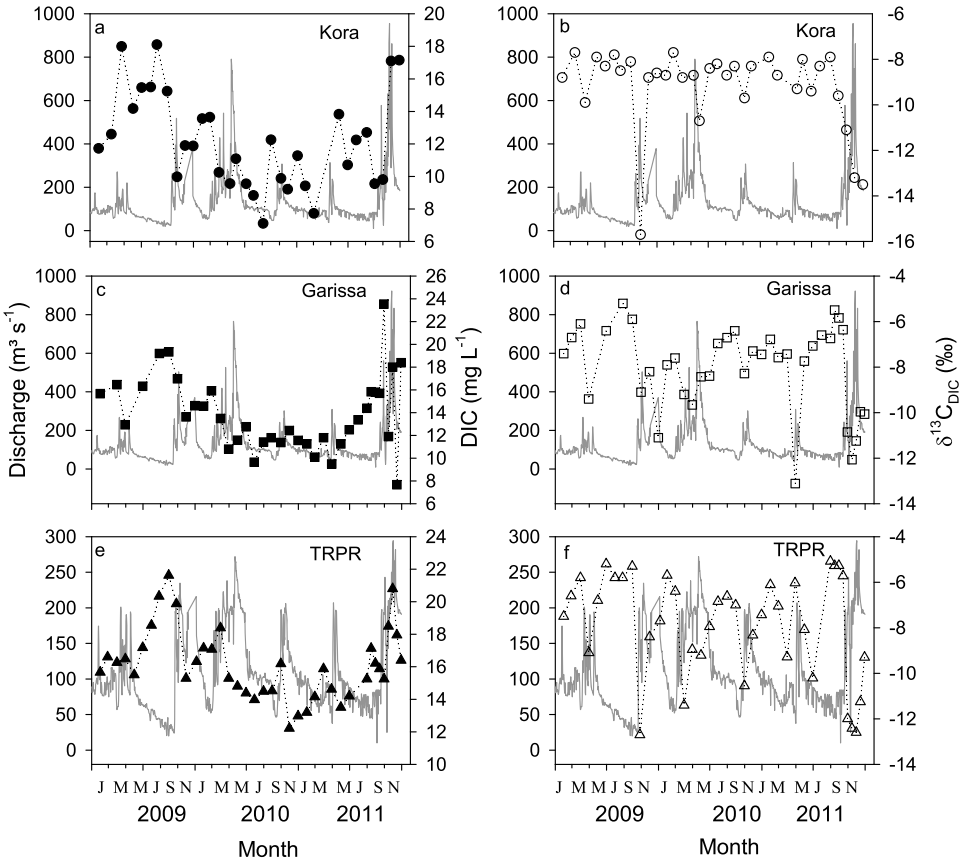

Figure 7. Seasonal variation of the daily discharge against (a, c, and e) DIC concentrations (b, d, and f) and seasonal variations of the daily discharge against $\delta^{13}C_{DIC}$ signatures at the three sampling sites (Kora = Kora Bridge, GRS = Garissa, and TRPR = Tana River Primate Reserve).

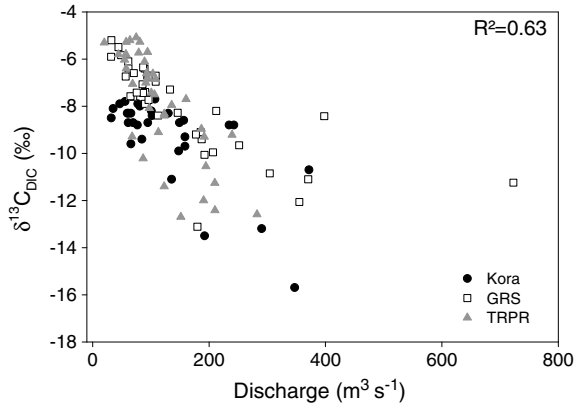

Figure 8. Relationship between $\delta^{13}C_{DIC}$ signatures against discharge at the three sampling sites (Kora = Kora Bridge, GRS = Garissa, and TRPR = Tana River Primate Reserve).

Bridge recording the highest value (9.2 ± 1.5), Garissa intermediate (7.9 ± 1.2), and TRPR the lowest mean (7.1 ± 0.9). The $\delta^{13}C_{POC}$ signatures ranged from −28.4‰ to −19.5‰ and showed a coinciding strong seasonal variability at all the three sites. The $\delta^{13}C_{POC}$ values increased markedly during the periods of high discharge and decreased toward the end of dry periods (Figure 5 and Table S1 in the supporting information). The $\delta^{13}C_{POC}$ signatures showed a positive correlation with discharge (Pearson's correlation, $p < 0.01$; $r^2 = 0.62$; Figure 6) with similar means across the three sites (−23.1 ± 1.6‰; ANOVA, $p > 0.05$).

In contrast to $\delta^{13}C_{POC}$, $\delta^{13}C_{DOC}$ signatures did not show any clear pattern with discharge despite exhibiting a wide variation (−27.2‰ to −17.4‰) over the hydrological cycle. The $\delta^{13}C_{DOC}$ signatures at TRPR were slightly depleted (−24.7 ± 1.8‰) compared to Kora Bridge (−23.0 ± 2.1‰) and Garissa (−23.7 ± 1.5‰). The $\delta^{13}C_{DIC}$ signatures ranged from −15.7‰ to −5.1‰ and showed a strong seasonal pattern at all sites with signatures decreasing markedly during high discharge and vice versa (Figure 7 and Table S1 in the supporting information). The $\delta^{13}C_{DIC}$ signatures showed a strong negative correlation with discharge at all sites (Pearson's correlation, $p < 0.01$; $r^2 = 0.63$; Figure 8).

3.3. Annual Mass Fluxes of Suspended Matter and Carbon

The loadings (mass transported per unit of time) and specific yields (mass transported per unit of time and unit of basin area) for TSM and different C pools are summarized in Table 1 and Figure 9, while the mean seasonal loads are presented in Figure 10. The estimates produced by the two methods (GUMLEAF and LOADEST) were highly comparable, although LOADEST generally predicted higher loadings. The relative difference between the two methods ranged from 4% to 39% (Table 1), and the largest deviation was obtained for the particulate fluxes (TSM and POC) at Kora Bridge (difference 32–39%). The mean annual TSM loading ranged from 3.2 to 8.7 Tg yr^{-1} over the period 2009–2011 across the three sampling sites.

Table 1. Annual Fluxes and Specific Yields of Suspended Matter and Carbon at Three Sampling Sites Along the Tana River[a]

			Annual Fluxes		Specific Yields		
			GUMLEAF Method	LOADEST Method	GUMLEAF Method	LOADEST Method	
Site	($m^3 s^{-1}$) Q	(km^2) Drainage Area	($Tg yr^{-1}$) TSM		($t km^{-2} yr^{-1}$) TSM		Rel. Diff. %
Kora Bridge	134	22,000	3.2	5.3	146.5	241.5	39
Garissa	132	35,000	5.9	8.7	169.4	247.7	32
TRPR	112	66,500	3.2	3.1	48.2	46.4	−4
			($Gg C yr^{-1}$)				
			POC		POC		
Kora Bridge			62.9	91.0	2.86	4.14	31
Garissa			92.5	104.9	2.64	3.00	12
TRPR			39.6	36.6	0.59	0.55	-8
			DOC		DOC		
Kora Bridge			12.7	13.9	0.58	0.63	9
Garissa			9.6	10.0	0.27	0.28	4
TRPR			6.0	6.5	0.09	0.10	8
			DIC		DIC		
Kora Bridge			50.6	60.4	2.30	2.75	16
Garissa			57.6	63.6	1.64	1.82	9
TRPR			56.4	62.2	0.84	0.94	9

[a]Two alternative estimates are calculated based on the GUMLEAF and LOADEST software programs (see text for details). Q: Discharge; Rel. Diff.: Relative difference.

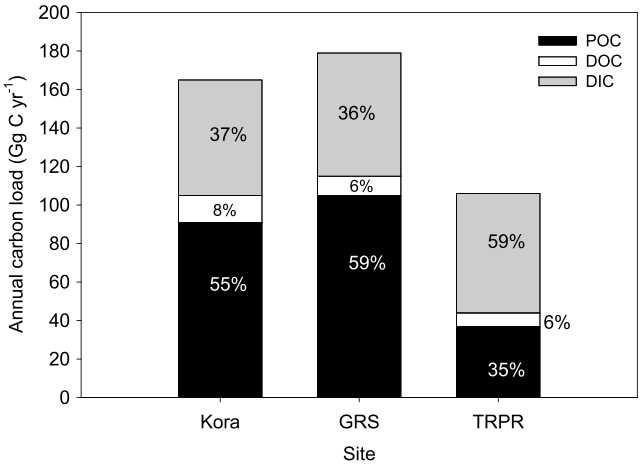

Figure 9. Annual carbon partitioning at the three sampling sites (Kora = Kora Bridge, GRS = Garissa, and TRPR = Tana River Primate Reserve).

The highest TSM and POC loadings were found at Garissa. On average, 84 ± 10% of the total TSM and 80 ± 12% of the total POC loads across all sites were exported during the high-flow period, i.e., from March to May and October to December (Figure 10a). The mean annual C fluxes ranged from 36.6 Gg C yr^{-1} to 104.9 Gg C yr^{-1}, 6.0 Gg C yr^{-1} to 13.9 Gg C yr^{-1}, and 50.6 Gg C yr^{-1} to 63.6 Gg C yr^{-1} for POC, DOC, and DIC, respectively (Table 1). In contrast to TSM, POC, and DOC fluxes, DIC fluxes did not show high variability between sampling sites (Table 1). The mean specific TSM yields ranged from 46.4 to 247.7 t km^{-1} yr^{-1} across the three sites over the period 2009–2011. Mean C specific yields ranged from 0.55 to 4.14 t C km^{-2} yr^{-1} for POC, 0.09 to 0.63 t C km^{-2} yr^{-1} for DOC, and 1.64 to 2.75 t C km^{-2} yr^{-1} for DIC (Table 1). The mean annual total C transport across all the sampling sites was partitioned as 49.2 ± 10.2% POC, 7.0 ± 1.8% DOC, and 43.8 ± 10.6% as DIC (Figure 9).

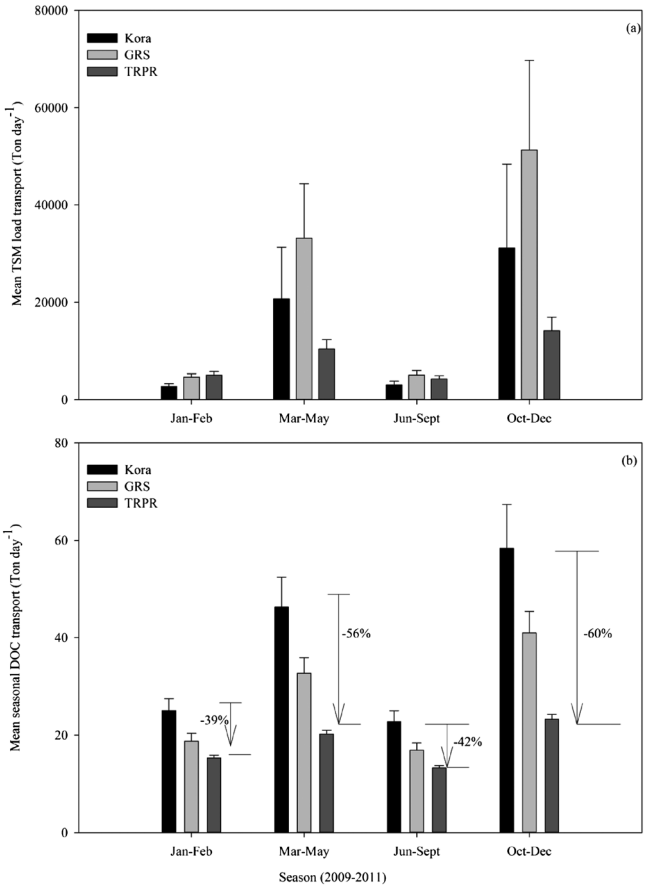

Figure 10. Seasonal loads of (a) TSM and (b) DOC at the three sites along the Tana River between 2009 and 2011.

4. Discussion

4.1. Suspended Matter and Organic Carbon Variability

The TSM and POC loads in any riverine system are a function of various factors such as climate, vegetation, topography, lithology, and discharge rate, in addition to various anthropogenic factors. The concentrations of both TSM and POC in the Tana River system are highly variable with maxima during or shortly preceding peak discharges (Figures 3 and 4), suggesting that the initial rains of the wet season mobilize surface soil layers and/or river bank sediments. As discharge continues to rise, the TSM and POC concentrations appear to decrease as indicated by the fact that the highest discharge rates do not show maximal sediment and POC loads (Figure 4), which is consistent with a sediment exhaustion effect [*Rovira and Batalla*, 2006; *Oeurng et al.*, 2011]. The TSM concentrations documented in the present study (range: 24–9386 mg L^{-1}) are relatively high compared to other African river systems, which range between 0.1 and 483 mg L^{-1} [*Coynel et al.*, 2005; *Bouillon et al.*, 2009, 2012], and are higher than the global average estimated at 500 mg L^{-1} [*Milliman and Farnsworth*, 2011].

Generally, %POC decreased during high flow, which is typical of most fluvial systems around the world [*Ludwig et al*., 1996; *Coynel et al*., 2005]. Low %POC in the Tana River system corresponded with high discharge and high TSM concentrations. These observations suggest that during high-discharge periods, mobilization of sediment occurs, which is characterized by a low organic content. In parallel with these seasonal changes in the %POC, $\delta^{13}C_{POC}$ signatures show distinct seasonal variations at all the three sampling sites, being relatively low (generally between −28‰ and −25‰) during low discharge conditions, but increasing markedly to values up to −19.5‰ during high-discharge periods. The ^{13}C-depleted values found during dry conditions are consistent with a dominant contribution of C derived from C3 vegetation such as direct input from riparian/riverine forest. In contrast, the higher $\delta^{13}C_{POC}$ values during high-discharge point toward a higher contribution of C derived from C4 vegetation. These low %POC, high-$\delta^{13}C$ inputs would be consistent with two sources (i) river bank erosion and/or (ii) surface soil erosion from areas more distant from the river channel. *Tamooh et al*. [2012] proposed that river bank erosion contributes significantly to the high-sediment loads in the lower main Tana. These river bank sediments are indeed characterized by a low organic content (0.4 ± 0.4%) [*Tamooh et al*., 2012] and relatively high $\delta^{13}C_{POC}$ signatures (usually in the range between −22 and −15‰) [*Tamooh et al*., 2012]. Mobilization of surface soils from more distant areas, where C4 grasslands or mixed savannah vegetation is more dominant, offer an alternative or complementary explanation. Soils in the lower region of the Tana Basin do in fact show relatively low OC contents and highly variable $\delta^{13}C$ [*Bouillon et al*., 2009; *Tamooh et al*., 2012]. Data on radionuclide activities in suspended sediments suggest that both processes contribute [*Tamooh et al*., 2012], but the current data set does not allow a more quantitative analysis of the relative importance of these two sources of suspended sediments and associated organic C.

Similar seasonal patterns in riverine $\delta^{13}C_{POC}$ have been reported from other catchments with mixed C3 and C4 vegetation [*Bird et al*., 1998; *Zhang et al*., 2009; *Marwick et al*., 2014], pointing toward a common driver behind the seasonal delivery of C3 versus C4-derived C to the river systems within tropical and subtropical latitudes.

Compared to suspended sediments and particulate OC loads, DOC shows much less pronounced variability during our 3 year study, although it must be noted that a substantial number of DOC samples were lost, and hence, the temporal coverage of our data set is less extensive. Nonetheless, DOC decreased significantly downstream (2.9 ± 1.1 mg C L^{-1} to 1.7 ± 0.3 mg C L^{-1}) and shows a flushing effect, with peak concentrations coinciding with high-flow regimes, particularly at Garissa and TRPR. This rapid response to increasing discharge suggests that DOC is primarily derived from terrestrial sources. In order to explain the downstream decrease in DOC, we considered the pelagic community respiration measurements made in the lower Tana River (1.92 μmol L^{-1} h^{-1}) [*Tamooh et al*., 2013] and extrapolated these to the estimated water transit time between Garissa and TRPR (5 days). This results in an estimated consumption of organic C (~2.75 mg C L^{-1}) between Garissa and TRPR which is several times higher than the 0.4 mg L^{-1} decline in DOC concentrations (from 2.1 ± 0.7 mg C L^{-1} to 1.7 ± 0.3 mg C L^{-1}). While pelagic respiration can be sustained by both particulate and dissolved OC, this calculation at least demonstrates that in situ riverine respiration is sufficiently high to account for the downstream DOC loss. The range of $\delta^{13}C_{DOC}$ (−27.2‰ to −17.4‰) reflects mixed contributions from both C3 and C4 vegetation and/or C3 and C4 vegetation dominated soils, although no systematic seasonal pattern could be discerned. The range of observed $\delta^{13}C_{DOC}$ signatures in the present study is wider than most African river systems [*Brunet et al*., 2009; *Bouillon et al*., 2012], suggesting temporal and spatial heterogeneity in DOC sources.

4.2. DIC Sources and $\delta^{13}C_{DIC}$ Dynamics

Various instream and watershed processes control riverine $\delta^{13}C_{DIC}$ signatures [*Amiotte-Suchet et al*., 1999; *Kandůc et al*., 2007], with primary controls being (i) the magnitude of photosynthesis and respiration (the former leading to a ^{13}C enrichment of the residual DIC pool and the latter introducing ^{13}C-depleted DIC with a signature close to the source of organic matter); (ii) the relative importance of carbonate and silicate weathering (silicate weathering adds DIC with a low-$\delta^{13}C$ signature similar to that of the organic matter producing the CO_2 which drives its dissolution, whereas carbonate weathering supplies DIC with higher signatures, intermediate between that of the carbonate and the CO_2 source); and (iii) the exchange of atmospheric CO_2 (with CO_2 outgassing leading to higher $\delta^{13}C_{DIC}$). Considering the high turbidity in the Tana River, photosynthesis is

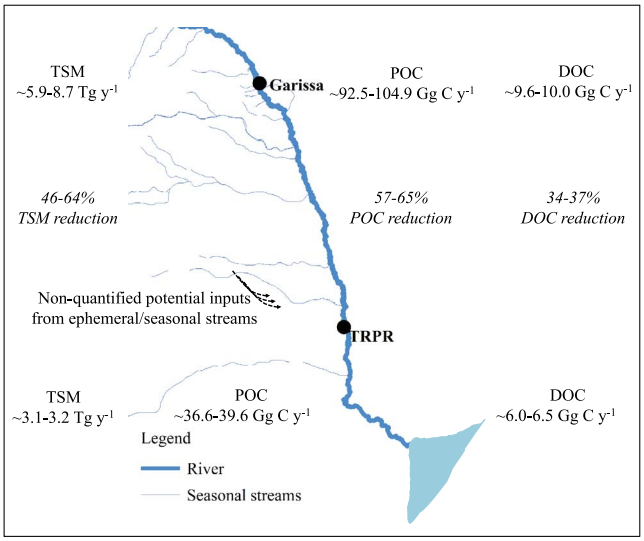

Figure 11. Schematic diagram showing the proportion of TSM and carbon retention along the Tana River between Garissa and TRPR.

unlikely to extert a strong influence. The seasonal variations that we observed in $\delta^{13}C_{DIC}$ signatures at the three stations in the lower main Tana (−15.7‰ to −5.1‰) nearly span the range observed over the whole Tana River basin (including headwaters) and other catchments [*Chakrapani and Veizer*, 2005; *Kandŭc et al.*, 2007; *Tamooh et al.*, 2013], which indicates that different regulating processes may be important across the hydrograph. The interplay of multiple controls and the absence of cation and Si concentration data, which could constrain the relative magnitude of carbonate and silicate weathering [*Tamooh et al.*, 2013], limit our ability to quantitatively constrain the different sources of DIC. However, $\delta^{13}C_{DIC}$ signatures were lower during high flows at all the three sites (Figure 7), resulting in a strong negative correlation between $\delta^{13}C_{DIC}$ signatures and discharge (Figure 8), and point toward different controls of DIC in base flow and peak discharge waters.

4.3. Annual Fluxes of Suspended Sediment and Carbon

While our data set represents to date the most detailed analysis of material fluxes in the Tana River system, we must stress that there is scope for further improvement, since (i) the monthly sampling resolution is still coarse compared to the rapid changes in discharge (Figures 2, 3, 5, and 7) and (ii) the daily discharge data were only available for one of the sites requiring extrapolations to the other two measurement stations. While sampling at higher temporal resolution and the establishment of new hydrological gauging stations are prerequisites in supplying more precise material flux estimates, the following discussion focuses on the downstream gradient in fluxes, and on the seasonality in observed fluxes, which should remain robust within the confines of the above considerations.

A comparison of the high-TSM load recorded at Garissa with those upstream and downstream (Table 1) indicates that (i) substantial mobilization of sediment occurs upstream between Kora and Garissa, while (ii) further downstream, a net reduction in the sediment flux occurs along the river stretch between Garissa and TRPR. Our annual TSM flux estimates at TRPR (3.1 to 3.2 Tg yr^{-1}; Table 1) are smaller than the 6.8 Tg yr^{-1} estimate previously reported by *Kitheka et al.* [2005] at Garsen, a site located ~80 km downstream of TRPR (Figures 1a and 1b). At the same time, the TSM concentration range observed here (between 66 and 5128 mg L^{-1}; $n = 40$) is larger than the one reported by *Kitheka et al.* [2005] (TSM concentration ranging between 530 and 1930 mg L^{-1}; $n = 19$). However, the *Kitheka et al.* [2005] TSM load estimate was based on a relatively small data set (19 sampling dates), and in addition, calculations were based on the average monthly discharges. These two issues can potentially bias flux estimates in systems with an irregular hydrograph. Our TSM load estimates at TRPR suggest substantial TSM retention (46% to 64%) in the downstream section of the lower main Tana between Garissa and TRPR, where substantial floodplains are present (Figure 11). Sediment retention could be even stronger, as our TSM balance does not account for TSM contributions from seasonal streams located between Garissa and TRPR, which are thought to be substantial [*Tamooh et al.*, 2012]. TSM load retention along the floodplains is particularly pronounced during high-flow regimes (Figure 10a). Similarly, annual POC fluxes showed a significant degree of retention (~57% to 65%; Figure 11), whereas no significant retention was observed for DIC (Table 1). A comparison of DOC fluxes shows that loadings consistently decrease downstream (13.9 Gg C yr^{-1} to 6.5 Gg C yr^{-1}; Table 1 and Figure 10b) and indicate a substantial loss of DOC (~34% to 37%) during downstream transit. The DOC reduction is similarly more pronounced during the high-flow regime (56 to 60% loss) than the low-flow regime (39% to 42% loss; Figure 10b), which could indicate rapid mineralization of fresh materials likely derived from terrestrial sources.

The overall mean sediment yield for Tana River across all sites is ~150 ± 89 t km^{-2} yr^{-1}. This value is relatively high compared to most African systems but approaches the mean global annual yield (190 t km^{-2} yr^{-1}) [*Milliman and Farnsworth*, 2011]. The mean pre-dam sediment yield of large African Rivers (Congo, Nile, Niger, Zambezi, and Orange, which collectively drain >40% of African continent) is 25 t km^{-2} yr^{-1}, whereas the mean predam yield of African semiarid rivers (Volta, Sanaga, Rufiji, Limpopo, and Senegal) is ~60 t km^{-2} yr^{-1} [*Milliman and Farnsworth*, 2011]. The overall mean POC yield in Tana River system (2.30 t C km^{-2} yr^{-1}; Table 1) is slightly higher than the global mean (1.6 t C km^{-2} yr^{-1}) [*Ludwig et al*., 1996]. In contrast, the average DOC yields (0.09 t C km^{-2} yr^{-1} to 0.63 t C km^{-2} yr^{-1}) across the three sites are relatively small compared to the global average (1.9 t C km^{-2} yr^{-1}) [*Ludwig et al*., 1996]. We attribute this to the generally organic-poor soils and the high temperature in lower Tana River basin [e.g., *Tamooh et al*., 2012], which is also consistent with the global observation that semi-arid regions typically have low river DOC concentrations [*Spitzy and Leenheer*, 1991].

Globally, the partitioning of riverine C fluxes between organic and inorganic, and between particulate and dissolved forms, differs significantly between climatic regions [*Ludwig et al*., 2011]. On average, around ~56% of the global riverine C transport flux is estimated to occur as inorganic C, the remaining 44% as organic C, in roughly equal quantities as POC and DOC [*Ludwig et al*., 1996; *Schlünz and Schneider*, 2000]. In tropical systems, river C fluxes are thought to be dominated by DOC (DOC > POC ≫ DIC). Our results for the Tana River show that this system differs from this general trend, with ~43% of the total C transported as DIC and ~57% as organic C, the latter being dominated by POC for which fluxes are 6–10 times higher than for DOC.

The substantial retention of sediments and organic C between Garissa and TRPR coincides with the presence of floodplains along this stretch of the river course and alludes to the key role that floodplains may play in regulating the downstream transport of riverine material. At present, quantification of this retention mechanism is poorly documented as only a few data sets exist [*Noe and Hupp*, 2009]. Moreover, while certain floodplains have been shown to act as sinks of riverine C, others are known to provide inputs of C to river systems. Global estimates suggest that ~50% of the organic C entering fluvial systems finally reaches the ocean [*Hope et al*., 1994; *Cole et al*., 2007]. Retention of riverine sediments is particularly high for large rivers with extensive floodplains and deltas [*Milliman and Farnsworth*, 2011]. Considering the high degree of material retention documented here for the lower Tana River, we propose that sediment retention within the river channel offers an improbable explanation, and the quantitative role of floodplains as the driving force behind sediment and organic C retention deserves more attention. If floodplains are indeed the primary sites of sediment and organic C retention, the fate of deposited C and the dynamics of the river bed (meandering rates and residence time of deposited sediments) will determine the time scales over which riverine C deposits are reintroduced in the aquatic environment.

Irrespective of the mechanisms, however, we can expect the total export of material to the coastal zone to represent only a small fraction of the overall terrestrial inputs to the Tana River and its tributaries, since significant sediment and organic C sinks are also known to occur both upstream (several hydroelectric reservoirs) and downstream of the area studied here (riverine floodplains downstream of TRPR and in the Tana delta). While the accuracy of Tana River load estimates could be refined in the future by higher-resolution temporal sampling and more accurate hydrological data, the first-order estimate provided here is crucial in recognizing the importance of suspended sediment retention along the lower main Tana River, between Garissa and TRPR, with riverine floodplains as the most obvious deposition zones. Previous basin-wide sampling campaigns [*Bouillon et al*., 2009; *Tamooh et al*., 2012] have typically shown a downstream increase in TSM during the dry season. Our seasonally partitioned sediment flux estimates for dry seasons (Figure 10a) similarly show a downstream increase (January–February) or relatively stable sediment flux (June–September). However, once integrated on an annual basis, the much larger fluxes during high-discharge periods dominate, resulting in an overall net reduction of sediment as well as particulate and dissolved organic C loads along this stretch of the river (Table 1 and Figures 10 and 11). We estimate that about 84% of the annual TSM transport and 80% of the annual POC transport occur during the high-discharge periods associated with the rain seasons. The clear seasonality in sediment and C retention suggests that a large interannual variability may occur in the degree to which material fluxes are retained along the lower Tana.

The five hydroelectric dams in the upper Tana Basin were commissioned between 1968 and 1988 [*Maingi and Marsh*, 2002]. The availability of historical data of sediment loads at Garissa [*Dunne*, 1988], prior to the

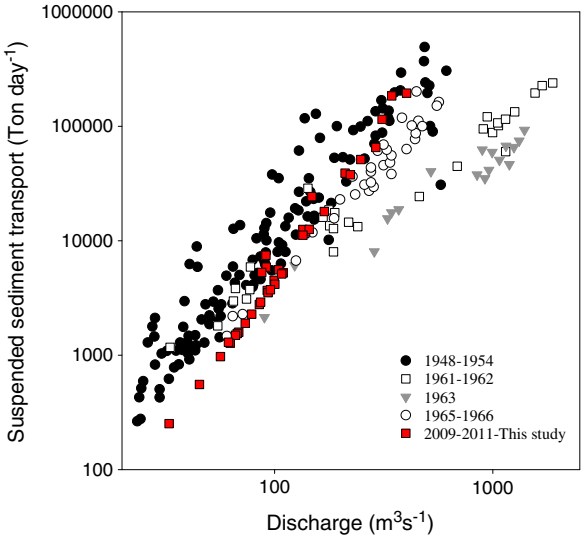

Figure 12. Comparisons of the Tana River total suspended matter transport and discharge rating curves at Garissa station before and after hydroelectric dam construction (dams commissioning done from 1968 to 1988). The historical data were obtained from *Dunne* [1988], and data from this study are calculated based on the discharge of sampling dates and the measured TSM concentration at these dates.

construction of these dams, allows a first assessment of decadal scale changes in sediment transport within the Tana Basin. At the lower end of the discharge range, a substantial reduction in the sediment load can be observed between pre-dam and postdam periods (Figure 12), consistent with the operation of the reservoirs as an effective sediment trap [*Dunne and Ongweny*, 1976; *Brown and Schneider*, 1998]. At intermediate discharge levels, however, such a reduction is no longer evident, suggesting less efficient trapping in the reservoirs and/or significant mobilization of sediments from areas downstream of the reservoirs. The latter would be consistent with our observation that sediment fluxes increase substantially between Kora and Garissa (Table 1 and Figure 10a) and earlier findings that a substantial mobilization of sediments occurs in this part of the lower main Tana, most likely due to bank erosion [*Tamooh et al.*, 2012]. Due to the prevailing flow control by hydropower dams, peak flows $>400\,m^3\,s^{-1}$ are less frequent and were missed by our sampling regime, making it difficult to compare the current situation with past scenarios (Figure 12). The Tana River would form an excellent case to investigate the longer-term effect of reservoirs on the sediment transport and sources in downstream river sections, but this would require more detailed flux studies or sediment flux reconstructions, as well as information regarding the origin of the sediments in the lower main Tana.

5. Conclusions

The fluxes of suspended sediments and different C pools were studied at the three sites along the lower Tana River (Kenya). Both TSM and POC deliveries were highly seasonal, with approximately 84% and 80% of their respective loads transported during the high-flow seasons (March to May and October to December) across all sites. The $\delta^{13}C$ data indicated that during high discharge, POC had mixed contributions of C3 and C4 vegetation, whereas during low discharge, POC was predominantly C3 derived and likely from within the riparian zone, i.e., riverine forest vegetation. In contrast, no such clear seasonality was evident for $\delta^{13}C_{DOC}$. While dry season longitudinal profiles show steady increases in sediment and POC concentrations downstream, our study shows that on an annual basis, there is a significant degree of retention of TSM, POC, and DOC along the lower Tana River, which is particularly pronounced during high-flow conditions. We propose that the presence of extensive floodplains along the river could play a key role in regulating the riverine transport, an issue which deserves further attention. Accounting for other sediment and C retention sites within the river basin (reservoirs upstream and floodplains downstream of the area studied here), our study demonstrates that the material transported by the Tana River to the coastal zone represents only a small fraction of the overall terrestrial inputs to the river system.

Acknowledgments

Funding for this work was provided by the Research Foundation Flanders (FWO-Vlaanderen, project G.0651.09 and travel grants to F.T., K.V.d.M., and S.B.) and the European Research Council (ERC-StG 240002, AFRIVAL-African river basins: catchment-scale carbon fluxes and transformations, http://ees.kuleuven.be/project/afrival/). A.V.B. is a research associate at the FRS-FNRS. We thank Zita Kelemen (KU Leuven), Michael Korntheuer (VUB) and Marc-Vincent Commarieu (ULg) for their technical and laboratory assistance, Peter Gitonga, Alfred Ngula, and Emmanuel Katana of the Kenya Wildlife Service for facilitating seasonal sampling, WRMA (Water Resource Management Authority) for making the discharge data from Garissa and Garsen available, and an anonymous reviewer and the Editor-in-Chief for their constructive comments on an earlier version of this manuscript.

References

Alin, S. R., R. Aalto, M. A. Goni, J. E. Richey, and W. E. Dietrich (2008), Biogeochemical characterization of carbon sources in the Strickland and Fly rivers, Papua New Guinea, *J. Geophys. Res.*, *113*, F01S05, doi:10.1029/2006JF000625.

Amiotte-Suchet, P., D. Aubert, J. L. Probst, F. Gauthier-Lafaye, A. Probst, F. Andreux, and D. Viville (1999), $\delta^{13}C$ pattern of dissolved inorganic carbon in a small granitic catchment: The Strengbach case study (Vosges mountains, France), *Chem. Geol.*, *159*, 129–145.

Bird, M. I., P. Giresse, and S. Ngos (1998), A seasonal cycle in the carbon isotope composition of organic carbon in the Sanaga River, Cameroon, *Limnol. Oceanogr.*, *43*, 143–146.

Bouillon, S., et al. (2009), Distribution, origin and cycling of carbon in the Tana River (Kenya): A dry season basin-scale survey from headwaters to the delta, *Biogeosciences*, *6*, 2475–2493.

Bouillon, S., A. Yambélé, G. M. Spencer, D. P. Gillikin, P. J. Hernes, J. Six, R. Merckx, and A. V. Borges (2012), Organic matter sources, fluxes and greenhouse gas exchange in the Oubangui River (Congo River basin), *Biogeosciences*, *9*, 2045–2062.

Brown, T., and H. Schneider (1998), From plot to basin: The scale problem in studies of soil erosion and sediment yield, in *The Sustainable Management of Tropical Catchments*, edited by D. Harper and T. Brown, pp. 21–30, John Wiley and Sons, Chichester, England.

Brunet, F., K. Dubois, J. Veizer, G. R. Nkoue Ndondo, J. R. Ndam Ngoupayou, J. L. Boeglin, and J. L. Probst (2009), Terrestrial and fluvial carbon fluxes in a tropical watershed: Nyong basin, Cameroon, *Chem. Geol.*, *265*, 563–572.

Cai, W. J., X. Guo, C. T. A. Chen, M. Dai, L. Zhang, W. Zhai, K. Yin, and P. J. Harrison (2008), A comparative overview of weathering intensity and HCO_3^- flux in the world's major rivers with emphasis on the Changjiang, Huanghe, Zhujiang (Pearl) and Mississippi Rivers, *Cont. Shelf Res.*, *28*, 1538–1549.

Chakrapani, G. J., and J. Veizer (2005), Dissolved inorganic carbon isotopic compositions in the Upstream Ganga river in the Himalayas, *Curr. Sci.*, *89*, 553–556.

Cole, J. J., et al. (2007), Plumbing the global carbon cycle: Integrating inland waters into the terrestrial carbon budget, *Ecosystems*, *10*, 171–184.

Coynel, A., P. Seyler, H. Etcheber, M. Meybeck, and D. Orange (2005), Spatial and seasonal dynamics of total suspended sediment and organic carbon species in the Congo River, *Global Biogeochem. Cycles*, GB4019, doi:10.1029/2004GB002335.

DHV (1986), Tana River Morphology Studies. Final Report. Volume 1 Main report. Delft Hydraulics Laboratory.

Dunne, T. (1988), Geomorphic contributions to flood control planning, in *Flood Geomorphology*, edited by V. R. Baker, R. C. Kochel, and P. C. Patton, pp. 421–438, John Wiley and Sons, New York.

Dunne, T., and G. S. O. Ongweny (1976), A new estimate of sedimentation rates on the upper Tana River, *Kenyan Geogr.*, *2*, 109–126.

Gillikin, D. P., and S. Bouillon (2007), Determination of $\delta^{18}O$ of water and $\delta^{13}C$ of dissolved inorganic carbon using a simple modification of an elemental analyzer – isotope ratio mass spectrometer (EA-IRMS): An evaluation, *Rapid Commun. Mass Spectrom.*, *21*, 1475–1478.

Hoffmann, T., S. Glatzel, and R. Dikau (2009), A carbon storage perspective on alluvial sediment storage in the Rhine catchment, *Geomorphology*, *108*, 127–137.

Hope, D., M. F. Billett, and M. S. Cresser (1994), A review of the export of carbon in river water: Fluxes and processes, *Environ. Pollut.*, *84*, 301–324.

Junk, W. J., P. B. Bayley, and R. E. Sparks (1989), The flood pulse concept in river-floodplain systems, in *Proceedings of the International Large Rivers Symposium (LARS)*, Can. Spec. Publ. Fish. Aquat. Sci., vol. 106, edited by D. P. Dodge, pp. 110–127, Dept. of Fisheries and Oceans, Ottawa, Canada.

Kandûc, T., K. Szramek, N. Ogrinc, and L. M. Walter (2007), Origin and cycling of riverine inorganic carbon in the Sava River watershed (Slovenia) inferred from major solutes and stable carbon isotopes, *Biogeochemistry*, *86*, 137–154.

Kitheka, J. U., M. Obiero, and P. Nthenge (2005), River discharge, sediment transport and exchange in the Tana estuary, Kenya, *Estuarine Coastal Shelf Sci.*, *63*, 455–468.

Ludwig, W., J. L. Probst, and S. Kempe (1996), Predicting the oceanic input of organic carbon by continental erosion, *Global Biogeochem. Cycles*, *10*, 23–41, doi:10.1029/95GB02925.

Ludwig, W., P. Amiotte-Suchet, J. L. Probst (2011), ISLSCP II Global River Fluxes of Carbon and Sediments to the Oceans, in *ISLSCP Initiative II Collection*, edited by F. G. Hall et al., Oak Ridge National Laboratory Distributed Active Archive Center, Oak Ridge, Tennessee, doi:10.3334/ORNLDAAC/1028, Data set. [Available on-line from http://daac.ornl.gov/.]

Maingi, J. K., and S. E. Marsh (2002), Quantifying hydrologic impacts following dam construction along the Tana River, Kenya, *J. Arid Environ.*, *50*, 53–79.

Marwick, T. R., A. V. Borges, K. Van Acker, F. Darchambeau, and S. Bouillon (2014), Disproportionate contribution of riparian inputs to organic carbon pools in freshwater systems, *Ecosystems*, doi:10.1007/s10021-014-9772-6.

Milliman, J. (2001), River Inputs, in *Encyclopedia of Ocean Sciences*, 2nd edn., edited by A. Thorpe and K. K. Turekian, pp. 2419–2427, Academic Press, New York.

Milliman, D. J., and L. K. Farnsworth (2011), *River Discharge to the Coastal Ocean: A Global Synthesis*, Cambridge, Cambridge Univ. Press.

Noe, B. G., and R. C. Hupp (2009), Retention of riverine sediment and nutrient loads by coastal plain floodplains, *Ecosystems*, *12*, 728–746.

Oeurng, C., S. Sauvage, A. Coynel, E. Maneux, H. Etcheber, and M. J. Sanchez-Perez (2011), Fluvial transport of suspended sediment and organic carbon during flood events in a large agricultural catchment in southwest France, *Hydrol. Processes*, *25*, 2365–2378.

Richey, J. E. (2004), Pathways of atmospheric CO_2 through fluvial systems, in *The Global Carbon Cycle: Integrating Humans, Climate, and the Natural World*, edited by C. B. Field and M. R. Raupach, pp. 329–340, Island Press, Washington, D. C.

Richey, J. E. (2006), Global river carbon biogeochemistry, in *Encyclopedia of Hydrological Sciences*, Chapter 113, vol. 3, edited by M. G. Anderson and J. J. McDonnell, pp. 1,733–1,740, John Wiley & Sons, New Jersey.

Rovira, A., and R. Batalla (2006), Temporal distribution of suspended sediment transport in a Mediterranean basin: The Lower Tordera (NE Spain), *Geomorphology*, *79*, 58–71.

Runkel, R. L., C. G. Crawford, and T. A. Cohn (2004), Load Estimator (LOADEST): A FORTRAN Program for estimating constituent loads in streams and rivers, USGS Report.

Schlünz, B., and R. R. Schneider (2000), Transport of terrestrial organic carbon to the oceans by rivers: Re-estimating flux- and burial rates, *Int. J. Earth Sci.*, *88*, 599–606.

Spitzy, A., and J. Leenheer (1991), Dissolved organic carbon in rivers, in *Biogeochemistry of Major World Rivers*, Scope, vol. 42, edited by E. T. Degens, S. Kempe, and J. E. Richey, John Wiley, Chichester.

Syvitski, J. P. M., and J. D. Milliman (2007), Geology, geography and humans battle for dominance over the delivery of fluvial sediment to the coastal ocean, *J. Geol.*, *115*, 1–19.

Tamooh, F., K. Van den Meersche, F. Meysman, F. Dehairs, R. T. Marwick, A. V. Borges, R. Merckx, S. Schmidt, J. Nyunja, and S. Bouillon (2012), Distribution and origin of suspended matter and organic carbon pools in the Tana River Basin, Kenya, *Biogeosciences*, *9*, 2905–2920.

Tamooh, F., A. V. Borges, F. J. R. Meysman, K. Van Den Meersche, F. Dehairs, R. Merckx, and S. Bouillon (2013), Dynamics of dissolved inorganic carbon and aquatic metabolism in the Tana River Basin, Kenya, *Biogeosciences*, *10*, 6911–6928, doi:10.5194/bg-10-6911-2013.

Tan, K. S., T. Etchells, and D. R. Fox (2005), GUMLEAF v0.1alpha: Generator for uncertainty measures and load estimates using alternative formulae, *Environmetrics Australia*, University of Melbourne.

Zhang, S. R., X. X. Lu, H. G. Sun, J. T. Han, and D. L. Higgitt (2009), Geochemical characteristics and fluxes of organic carbon in a human-disturbed mountainous river (the Luodingjiang River) of the Zhujiang (Pearl River), China, *Sci. Total Environ.*, *407*, 815–825.

Zurbrügg, R., S. Suter, M. F. Lehmann, B. Wehrli, and D. B. Senn (2013), Organic carbon and nitrogen export from a tropical dam-impacted floodplain system, *Biogeosciences*, *10*, 23–38, doi:10.5194/bg-10-23-2013.